

Temperature Effects on Electron Transfer within Intervalence Bis(Hydrazine) Radical Cations

Stephen F. Nelsen,* Rustem F. Ismagilov, Kevin E. Gentile, and Douglas R. Powell

Contribution from the Department of Chemistry, University of Wisconsin, 1101 University Avenue, Madison, Wisconsin 53706-1396

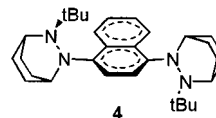
Received November 23, 1998. Revised Manuscript Received May 24, 1999

Abstract: Analyses of the shape of intervalence charge-transfer bands at various temperatures (~255–325 K in most cases) in acetonitrile are reported for the radical cations of bis(2-*tert*-butyl-2,3-diazabicyclo[2.2.2]-oct-3-yl) hydrazines that are bridged by 2,5-xylene-1,4-diyl (**2**⁺), durene-1,4-diyl (**3**⁺), naphthalene-1,4-diyl (**4**⁺), biphenyl-4,4'-diyl (**5**⁺), and 9,9-dimethylfluorene-2,7-diyl (**6**⁺) aromatic rings. Electron-transfer (ET) rate constants measured by ESR as a function of temperature are reported for **4**⁺–**6**⁺. Despite the fact that the ET barriers for these compounds are dominated by vibrational reorganization, explicit inclusion of vibronic coupling effects is not necessary for the prediction of their ET rate constants from the optical spectra. Rate constants in excellent agreement with the measured ones are predicted by a classical analysis of charge-transfer band shape, if the diabatic surfaces are changed from the usual assumption that they are parabolas to ones that fit the shape of the charge-transfer bands.

Introduction

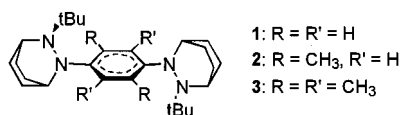
Charge-localized symmetrical intervalence (IV) compounds provide the simplest electron-transfer (ET) systems to consider.¹ They have two identical charge-bearing units (CBU) attached to a Bridge, and are at an oxidation level that places different charges on the CBU. The ones considered here have easily oxidized (Donor) CBU, and may be symbolized as **D-B-D**⁺. When the electronic coupling between the CBU through the bridge connecting them (measured by Hush's matrix coupling element *V*) is large enough, IV compounds show a charge-transfer (CT) optical band from which the rate constant for thermal intramolecular ET (*k*_{ET}) may be estimated using Marcus–Hush theory.^{2,3} The system is always at equilibrium because the driving force for ET is zero in symmetrical IV–CT compounds, and with most charge-bearing units, the ET rate constant is too large to measure when *V* is large enough that the optical band is easy to study. We have prepared examples with high internal reorganization energy hydrazine CBU that slow ET enough to allow *k*_{ET} to be measured by dynamic electron spin resonance (ESR). The first aromatic-bridged bis(hydrazine) IV compound we made, **1**⁺ (bridge abbreviation, **PH**, for phenylene-1,4-diyl), had *k*_{ET} values too

bridge in **2**⁺ (**XY**lene-1,4-diyl) and **3**⁺ (**DU**rene-1,4-diyl) increases the twist angle (ϕ) between the nitrogen lone pair and the bridge π system, lowering *V* enough that *k*_{ET} can be determined.⁵ Another way of increasing ϕ is by introducing a benzo group on the bridging ring, and we report here studies on the 1,4-naphthalene-bridged compound **4**⁺. Adding a second



benzo group to give the 9,10-anthracene-bridged compound further increases ϕ but significantly changes the character of its intramolecular ET. As discussed elsewhere,⁶ there is a large increase in *k*_{ET}, the IV–CT band is obscured by a bridge oxidation band, and this IV compound cannot reasonably be treated as a simple two-state Marcus–Hush system such as the compounds discussed here.

In this work we also increase the bridge length from the 5- σ -bonds bridging the hydrazine units of **1**⁺–**4**⁺ to the nine of the biphenyl (**5**⁺, **PH**₂) and 9,9-dimethylfluorenyl-bridged compound (**6**⁺, **M**₂**FL**). Increasing the distance decreases *V* enough⁷



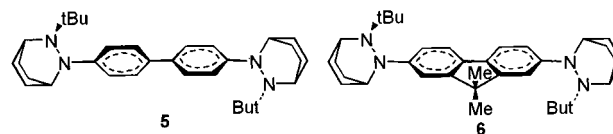
large to measure accurately.⁴ Introducing methyl groups on the

(1) For reviews of transition metal-centered IV compounds see (a) Creutz, C. *Prog. Inorg. Chem.* **1983**, *30*, 1. (b) Crutchley, R. *J. Adv. Inorg. Chem.* **1994**, *41*, 273.

(2) (a) Hush, N. S. *Prog. Inorg. Chem.* **1967**, *8*, 391. (b) Hush, N. S. *Coord. Chem. Rev.* **1985**, *64*, 135.

(3) (a) Sutin, N. *Prog. Inorg. Chem.* **1983**, *30*, 441. (b) Marcus, R. A.; Sutin, N. *Biochim. Biophys. Acta* **1985**, *811*, 265.

(4) Nelsen, S. F.; Ismagilov, R. F.; Powell, D. R. *J. Am. Chem. Soc.* **1996**, *118*, 6313.



to allow ESR rate studies without the larger ϕ provided by including ortho substituents. ESR rate constants for **2**⁺–**6**⁺ may only be determined in the relatively narrow temperature range

(5) Nelsen, S. F.; Ismagilov, R. F.; Powell, D. R. *J. Am. Chem. Soc.* **1997**, *119*, 10213.

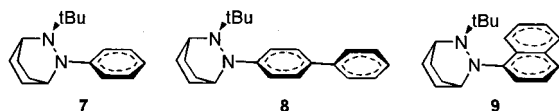
(6) Nelsen, S. F.; Ismagilov, R. F. *J. Am. Chem. Soc.* **1998**, *120*, 1924.

(7) For discussion of how *V* varies as bridge size is increased for delocalized diamino-aromatic cation radicals, see Nelsen, S. F.; Tran, H. Q.; Nagy, M. A. *J. Am. Chem. Soc.* **1998**, *120*, 298.

where k_{ET} is within a factor of about three of $10^8 \text{ M}^{-1} \text{ s}^{-1}$, making experimental values (k_{ESR}) only available at different temperatures for different compounds. In this work we report optical studies on $2^+–6^+$ in acetonitrile, where ion pairing effects are negligible,⁸ at temperatures that vary over a $\sim 70^\circ$ range centered near room temperature. These data allow more direct comparison of the thermal and optical rate constants than the room temperature optical measurements previously available.⁹

Results

Compounds **4–6** were prepared by double addition of 2-*tert*-butyl-2,3-diazabicyclo[2.2.2]oct-3-enium tetrafluoroborate to the dilithio aromatic, as previously described⁵ for **1–3** (see experimental). In contrast to successful crystal structure determination for the intervalence oxidation-state salts of 1^+ and 3^+ ,⁵ we were unable to obtain one of 5^+ , which disproportionated upon all attempts at isolation, probably because V for 5^+ is significantly smaller, making it less stable relative to **5** and 5^{2+} . The structure we obtained for 5^0 is not very good, both because of disorder problems (the crystal contained 83% of a *syn* isomer lying on a crystallographic center of inversion and 17% of another with the opposite lone pair, aryl twist angle, so only data for the major isomer have much precision) and because the rotational angle between the *p*-phenylene groups (ψ) obtained for both isomers was 0° . Although it is common for crystal structures of biphenyl derivatives to give $\psi = 0$ values, it has been pointed out that this can occur because ψ is incommensurate with the unit cell used or because of the very flat energy surface for twisting about the central bond¹⁰ and does not really mean that $\psi = 0$ in the crystal. The crystal obtained for $5^{2+}(\text{SbF}_6^-)_2$ contained one molecule of acetonitrile in the unit cell. It has $\psi = 35.4(8)^\circ$, and the 5^{2+} unit does not lie on a crystallographic center of symmetry, so the two hydrazine units are crystallographically independent. The distance between the arylated nitrogens of 5^0 and 5^{2+} was 10.05 and 9.90 Å, respectively, to be compared to the 5.66–5.71 Å distances obtained for various oxidation states of **1–3**.⁵ The ET distances d used in extracting V below were estimated from the dipolar splittings of the triplet states of 2^{2+} , 3^{2+} , and 5^{2+} as previously described.⁵ Changes in the twist angle ϕ affect the ET parameters, and we tried to study them using model compounds. The ϕ obtained for the major isomer of 5^0 was $42.9(4)^\circ$, somewhat larger than the $(-)-37.5^\circ$ obtained for 1^0 .⁵ The ϕ values for 5^{2+} , $(-)-44.1(8)^\circ$ and $(-)-43.9^\circ$, are significantly smaller than for either the phenyl monohydrazine radical cation analogue 7^+NO_3^- ($(-)-59.2^\circ$) or the cationic end of 1^+BF_4^- ($(+)-47.6(3)^\circ$).⁵ We also obtained the crystal structure of 8^+SbF_6^- , which gave $\phi = +53.3(6)^\circ$,



so the ϕ obtained for 5^{2+} appears anomalously small and may well represent an effect of crystal-packing forces. The crystal structure of 9^+SbF_6^- was determined as a model for twist in 4^+ and gave $\phi = (+)64.7(9)^\circ$, larger than the $(+)-57.4(2)^\circ$ obtained for $2^{2+}(\text{BF}_4^-)_2$, but comparable to that for $3^{2+}(\text{BPh}_4^-)_2$, $(-)-63.6(4)^\circ$, and the cationic end of $3^+(\text{BPh}_4^-)$, $(-)-66.2(3)^\circ$.⁵

(8) Nelsen, S. F.; Ismagilov, R. F. *J. Phys. Chem. A* **1999**, *103*, in press.

(9) Nelsen, S. F.; Ismagilov, R. F.; Trieber, D. W., II *Science* **1997**, *278*, 846.

(10) (a) Baudour, J. L. *Acta Crystallogr., Sect. B* **1991**, *47*, 935. (b) Etrillard, J.; Toudic, B.; Cailleau, H.; Goddens, G. *Phys. Rev. B* **1995**, *51*, 8733.

Table 1. IV-CT Band Data for Aromatic-Bridged Bis(hydrazine) Cations in Acetonitrile

cmpd	bridge	T (K)	E_{op} (cm ⁻¹)	ϵ_{max}^a	$\Delta\nu_{1/2}^b$ (cm ⁻¹)	C	λ^c	$V_H^{c,d}$	ΔG^*^c
1^{+5}	PH	~295				0.11 ₅	37.8	7.18	2.98
2^+	XY	255	14480	2226	5810	0.06	41.5	4.85	5.68
		270	14430	2177	5930	0.05 ₅	41.4 ₅	4.84	5.68
		284	14380	2133	6070	0.05 ₅	41.3	4.84	5.65
		298	14330	2100	6210	0.05 ₅	41.1 ₅	4.85	5.61
		312	14270	2074	6330	0.05 ₅	41.0	4.86	5.57
		327	14230	2064	6430	0.05	40.8 ₅	4.88	5.55
3^+	DU	255	14260	1030	6920	0.22	41.1 ₅	3.32	5.85
		270	14210	1010	7040	0.21	40.9 ₅	3.31	5.86
		284	14160	990	7170	0.20 ₅	40.8	3.30	5.89
		298	14110	970	7290	0.20	40.6 ₅	3.29	5.92
		312	14050	955	7370	0.19	40.5	3.28	5.90
		326	13995	942	7490	0.18 ₅	40.3 ₅	3.27	5.9
4^+	NA	255	12870	2250	5030	0.00	36.80	4.28	5.42
		270	12800	2204	5160	0.00	36.60	4.28	5.37
		284	12750	2165	5285	0.00	36.45	4.29	5.34
		298	12680	2127	5395	0.00	36.25	4.28	5.29
		312	12630	2091	5510	0.00	36.10	4.28	5.25
		327	12570	2069	5670	0.00 ₅	35.95	4.31	5.16
5^+	PH ₂	256	15410	2868	6000	0.06	44.2	3.79	7.12
		270	15340	2877	5990	0.04	43.9	3.72	7.25
		284	15290	2686	6040	0.03	43.7 ₅	3.67	7.34
		298	15210	2600	6090	0.01 ₅	43.5	3.60	7.45
		312	15170	2544	6130	0.01	43.4	3.58	7.48
		326	15110	2505	6160	0.00	43.2	3.56	7.53
6^+	M ₂ FL	255	13700	3980	4950	-0.03	39.1	4.08	6.35
		270	13630	3860	5080	-0.03	38.9	4.06	6.31
		284	13610	3770	5250	-0.02 ₅	38.8 ₅	4.08	6.25
		298	13555	3700	5370	-0.02 ₅	38.7	4.08	6.21

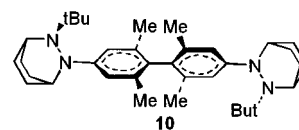
^a Units: $\text{M}^{-1} \text{ cm}^{-1}$. ^b From band simulation chosen to fit the low-energy side of the band as well as possible. ^c Units: kcal/mol. ^d ET distances (d , Å) used in calculating V_H : 1^+ 4.6; 2^+ 5.25; 3^+ 5.657; 4^+ 5.25; 5^+ 8.0; 6^+ 7.5.

Table 2. ESR Rate Constants for $4^+–6^+$ in Acetonitrile

$4^+(\text{NA})$		$5^+(\text{PH}_2)$		$6^+(\text{M}_2\text{FL})$	
T (K)	k_{ESR}^a	T (K)	k_{ESR}^a	T (K)	k_{ESR}^a
223 ^b	1.85	328.1	1.34	248.1	1.06
229	2.11	333.1	1.48	253.1	1.25
233	2.42	338.1	1.63	258.1	1.50
238	2.73	343.1	1.76	268.1	2.07
243	3.04	348.1	1.94	273.1	2.42
		353.1	2.11		

^a Units: 10^8 s^{-1} . ^b Although below the temperature for pure solvent freezing, these solutions had not frozen.

Optical data for the IV-CT bands of $2^+–6^+$ collected between ~ 255 and 327 K are summarized in Table 1. ESR rate constants for $4^+–6^+$ as a function of temperature were determined as previously described for 2^+ and 3^+ ⁵ and are summarized in Table 2. The tetramethylbiphenylene-bridged compound 10^+ was also prepared and studied to provide a



compound with a greatly twisted biphenyl bridge and to allow consideration of the effect of the twist angle of the biphenyl ring (ψ) on k_{ET} . No IV-CT band was observed for 10^+ (no significant attempt was made to find a weak band, but ϵ is clearly $< 200 \text{ M}^{-1} \text{ cm}^{-1}$), nor was any ESR line broadening corresponding to k_{ESR} approaching $7 \times 10^7 \text{ s}^{-1}$ observed as the temperature was raised.

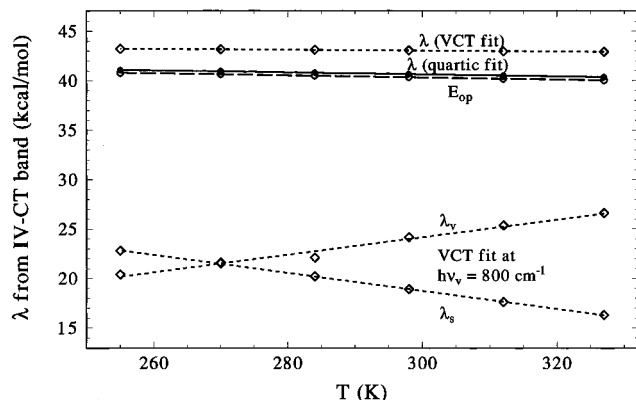


Figure 1. Comparison of λ values derived from the intervalence charge-transfer band of 3^+ in acetonitrile using classical and vibronic coupling theory.

Discussion

Optical IV–CT Band Simulation. Classical Marcus–Hush theory uses a two-state treatment with V as the off-diagonal matrix element generating adiabatic energy surfaces from diabatic surfaces that are parabolas placed at zero and one on an ET coordinate (X) that includes both solvent and internal vibrational reorganizational energy.^{2,3} The transition energy at the IV–CT band maximum (E_{op}) is equal to the total vertical reorganization energy (λ), and V has traditionally been calculated using Hush’s equation 1,

$$V_H = [0.0206/d][E_{op}\Delta\nu_{1/2}\epsilon_{max}]^{1/2} \quad (1)$$

where d is the electron-transfer distance, $\Delta\nu_{1/2}$ is the bandwidth at half-height, and ϵ_{max} is the extinction coefficient at the band maximum. Fitting the IV–CT band is necessary for reasonably accurate estimation of bandwidth at half-height ($\Delta\nu_{1/2}$) to allow accurate estimation of V_H , because varying amounts of overlap with other bands on the high-energy side of the IV–CT band make reading ϵ for the IV–CT off the recorded spectrum on this side unreliable. Classical Marcus–Hush theory produces Hush’s “high temperature limit” (HTL) bandwidth, shown in eq 2.

$$\Delta\nu^{HTL} = [16RT\ln(2)E_{op}]^{1/2} \quad (2)$$

Equation 2 gives $\Delta\nu^{HTL} = 5390$ to 5960 cm^{-1} at 298 K for E_{op} values in the range studied, but several of the observed bandwidths are significantly broader. Hush assumed that the larger bandwidth often observed arises from tunneling effects when the averaged barrier-crossing frequency ($h\nu_v$) is larger than $2k_B T$, as it certainly is for our compounds.

In more recent papers, a vibronic coupling theory treatment is usually employed.¹¹ The Marcus–Hush ET coordinate is replaced by a new one (Y) that includes only low-frequency reorganization (usually described as solvent reorganization), and the internal vibrational reorganization is treated by calculating Franck–Condon factors for vertical transitions between a parabolic $i = 0$ vibrational level of the initial state (centered at $Y = 0$) and each vibrational level j in a nest of parabolas separated by $h\nu_v$ at $Y = 1$ for the final state (see Figure 1 from

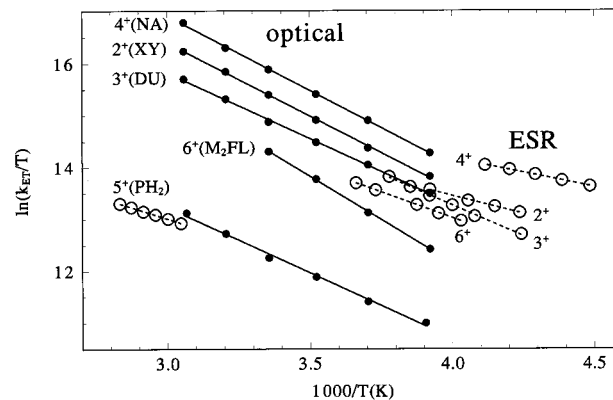


Figure 2. Eyring plots comparing optical (filled circles) and ESR (empty circles) rate constants for 2^+ – 6^+ in acetonitrile.

ref 12 a for a diagram). The Kodak group was the first to fully apply vibronic coupling theory to absorption bands,¹³ although aspects of such a treatment are included in Hush’s early analysis.^{2a} We have applied the vibronic coupling theory treatment to optical bands of σ -bridged bis(hydrazine) and bis-(diazonium) radical cations,^{12a,b} as well as 1^+ – 3^+ ,^{12c} and pointed out that simulation of the bands does not allow separation of the three ET parameters required for vibronic coupling theory (the averaged energy of the barrier-crossing frequency, $h\nu_v$, and the solvent and vibrational reorganization energies, λ_s and λ_v) and that k_{ET} values that are smaller and have larger variation with temperature than those observed are obtained from such a treatment. We suggested that the main problem with using vibronic coupling theory for our compounds is their very large λ_v values.^{5,12} The λ_v and $h\nu_v$ values estimated for hydrazines used with a single averaged $h\nu_v$ ^{11,13} would require that the vibrational energy surfaces remain harmonic to $j > 11$, which seems exceedingly unlikely. The result of using a vibronic coupling theory analysis of the optical spectrum of 3^+ as a function of temperature is shown graphically in Figure 1. When a constant $h\nu_v$ of 800 cm^{-1} (that used in our previous work)^{5,7} is employed over the 72° temperature range studied, the partitioning of λ into λ_s and λ_v changes substantially with temperature, λ_v increasing 30% as the temperature is raised, which seems physically unreasonable. Possibly an increasing fraction of the low-frequency components of λ_v should be transferred to λ_s (the Y coordinate) as $k_B T$ increases and a constant $h\nu_v$ should not be assumed. However, choosing $h\nu_v$ would then require complete knowledge of the distribution of $h\nu_v$ values and their contribution to λ_v , and such detailed information is not available. We cannot tell how to accurately partition λ into λ_s and λ_v at any temperature, and this information is crucial for applying vibronic coupling theory.

The experimental estimate of V , V_H , is determined by the transition dipole of the IV–CT band, included in eq 1. The size of V_H obtained is not significantly affected by using eq 1 to evaluate it, despite the differences in observed band shape from that predicted using parabolic diabatic surfaces. Predicting the thermal ET rate constant from optically derived parameters (k_{OPT}) requires obtaining the size of the ET barrier on E_1 (ΔG^*). The size of ΔG^* that arises from E_{op} and V_H depends significantly on the exact shape of the adiabatic surface. To accurately estimate ΔG^* , we therefore returned to the simple analysis of the IV–CT band using the merged λ_s, λ_v coordinate X of classical Marcus–Hush theory but relaxed the requirement that the diabatic surfaces are exactly parabolas. Because the ET

(11) (a) Jortner, J.; Ulstrup, J. *J. Chem. Phys.* **1975**, *63*, 4358. (b) Jortner, J.; Bixon, M. *J. Chem. Phys.* **1988**, *88*, 167. (c) Cortes, J.; Heitele, H.; Jortner, J. *J. Phys. Chem.* **1994**, *98*, 2527.

(12) (a) Nelsen, S. F.; Ramm, M. T.; Wolff, J. J.; Powell, D. R. *J. Am. Chem. Soc.* **1997**, *119*, 6863. (b) Nelsen, S. F.; Trieber, D. A., II.; Wolff, J. J.; Powell, D. R.; Rogers-Crowley, S. *J. Am. Chem. Soc.* **1997**, *119*, 6873.

(13) Gould, I. R.; Noukakis, D.; Gomez-Jahn, L.; Young, R. H.; Goodman, J. L.; Farid, S. *Chem. Phys.* **1993**, *176*, 439.

Table 3. Comparison of k_{OPT} Values Calculated by Fit of the IV-CT Band of 3^+ (DU) in Acetonitrile at 298 K Using Various Functions for H_{aa}

fitting term ^a	relative k_{OPT}^b	C_i
$C_3 X ^3$	0.995	0.315
$C_5 X ^5$	0.89	0.147
$C_{\text{exp}}\{(\exp X^2 - 1)/(e - 1)\}$	0.86	0.49
C_6X^6	0.72	0.12

^a The quartic fit uses eq 3, $H_{\text{aa}} = \lambda/(1 + C) [X^2 + CX^4]$. The other fitting functions replace the underlined term by that shown in the first column, and the corresponding C in the normalization term. ^b k_{OPT} (using the fitting term shown)/ k_{OPT} using eq 3 = $8.57 \times 10^8 \text{ s}^{-1}$, $C = -0.20$.

coordinate X is complex for multiatom systems, we suggest that there is no requirement that the changes in energy as the ET proceeds map onto X exactly as parabolas.^{5,8} In the simple two-state model, the relative extinction coefficient (ϵ_{rel}) at a given photon energy ($h\nu$) is determined by the Boltzmann factor: $\epsilon_{\text{rel}} = \epsilon(h\nu)/\epsilon_{\text{max}} = \exp(-\Delta E_1/RT)$. The energy separation between the ground-state energy surface and the excited-state surface is $h\nu$, and ΔE_1 is the increase in energy on E_1 relative to the minimum energy: $\Delta E_1 = E_1(h\nu) - E_{1,\text{min}}$. When the diabatic surfaces are parabolas, the bandwidth is given by eq 2. If the IV-CT band is broader than $\Delta\nu^{\text{HTL}}$ of eq 2, the diabatic surfaces are not exactly parabolas. A larger bandwidth is obtained when the diabatic surface as a function of X is broader near $X = 0$ but steeper near $X = 1$ than for parabolas. The IV-CT band shape for all of the compounds we have studied may be successfully simulated using quartic-augmented diabatic energy surfaces, that is, using eq 3.^{5,8}

$$H'_{\text{aa}} = \{\lambda/(1 + C)\}\{X^2 + C(X)^4\} \quad (3a)$$

$$H'_{\text{bb}} = \{\lambda/(1 + C)\}\{(X - 1)^2 + C(X - 1)^4\} \quad (3b)$$

For a comparison of observed and simulated band shape of $1^+ - 3^+$, see ref 5, Figure 3. When $C = 0$, the Marcus-Hush parabolic diabatic energy surfaces ($H_{\text{aa}} = \lambda(X)^2$, $H_{\text{bb}} = \{\lambda(X - 1)^2\}$) are obtained. A good fit to the observed bands is achieved using eq 3 as using vibronic coupling theory, consistent with the large interaction between λ_s , λ_v , and $h\nu_v$ noted in previous work.^{5,12} If λ and C (two parameters) can be adjusted to fit the IV-CT bands, the three parameters of vibronic coupling theory cannot be reliably extracted from these bands.

The thermal ET barrier ΔG^* is the increase in ground-state energy at the E_1 maximum (required by symmetry to occur at $X = 0.5$ for these systems) from that at the minimum ($E_{1,\text{min}}$). Good fit to the optical band is found using eq 3 for $\epsilon/\epsilon_{\text{max}} = 1$ down to 0.2 or less on the low-energy side for all of our compounds. This requires that ΔE_1 and the ground-state-excited-state energy gap ($h\nu$) are simultaneously reproduced between $X \sim 0$ and 0.15 and between ~ 0.85 and 1.0. Calculating ΔG^* requires only an interpolation of ΔE_1 to $X = 0.5$. Numerical solution for the adiabatic surfaces was used to calculate the optical ΔG^* values of Table 1, but these numbers are very close to that given by eq 4,

$$\Delta G^*(\text{using eq 3}) \cong (\lambda/4)(1 + C/4)/(1 + C) - V + V^2/\lambda \quad (4)$$

which is simply the solution for parabolas,² adjusted for the lower diabatic curve crossing by the $(1 + C/4)/(1 + C)$ term. We emphasize here that the functional form of H_{aa} that is used to fit the IV-CT band is not important for estimating ΔG^* , and hence k_{OPT} . As shown in Table 3, k_{OPT} values very close to those obtained using eq 3 are calculated when the IV-CT band is fit using H_{aa} functions that contain other powers of X or an

exponential term in X^2 , although the C_i coefficients vary depending on the function of X added to obtain fit to the optical spectrum. Fit to the optical spectrum becomes noticeably poorer when an X^6 term is added, and deviation of k_{OPT} values obtained are noticeably larger than they are using the other functions. Fit at the other temperatures studied using all of these H_{aa} fitting functions is similar, and lines in an Eyring plot of $\ln(k_{\text{OPT}}/T)$ vs $1/T$ are parallel using these functions. There is therefore no physical meaning in using specifically the X^4 additional fitting term in H_{aa} shown in eq 3; $|X|^3$, $|X|^5$ and the exponential X^2 term predict extremely similar barriers. It is significant that several functions that properly fit the CT band produce very similar ΔG^* values. We conclude that fitting the IV-CT band shape using classical theory as outlined above does allow prediction of the ET barrier. For simplicity, fits using eq 3 were used for all the spectra reported in Table 1.

Dependence of V on ψ for Biphenylene-Bridged Compounds. Electron transfers between the hydrazine units of the biphenylene-bridged bis(hydrazines) 5^+ , 6^+ , and 10^+ make an interesting contrast with those between zinc and Fe^{III} (imidazole)₂ porphyrin rings of the photoexcited arylene-bridged bis(porphyrins) studied by McLendon and co-workers.¹⁴ They determined ET rate constants using the usual assumption that zinc porphyrin fluorescence quenching rate constants may be equated with k_{ET} for these systems. The porphyrin rings are nearly perpendicular to the bridge rings ($\phi \sim 90^\circ$), causing very low V values, and consequently, strongly nonadiabatic ET reactions, for which $k_{\text{ET}} \propto V^2$. Changing from the **PH**- to the **PH**₂-bridged bis(porphyrin) system causes a slightly larger drop in effective V than for $1^+ \rightarrow 5^+$. The fluorescence quenching rate constant ratio for the bis(porphyrin) excited states is 5.7,^{11c} implying a V ratio of 2.4, compared with the V_{H} ratio obtained from the optical spectra of $1^+ \rightarrow 5^+$ of 2.02. The dependence of V upon ψ for biphenyl-bridged systems having porphyrin and hydrazine CBU is, however, quite different. ET rate constants between porphyrins were predicted considering only through space interactions to be at a maximum when the porphyrin rings are parallel or perpendicular and to reach a minimum at 45° twist¹⁵ and observed to be faster for substituted biphenyl-bridged bis(porphyrins) that have ψ at 0° and 90° than for species with intermediate angles, although the range k_{et} values reported is only a factor of 4.5.^{14c} In contrast, both k_{ESR} and V_{H} values for biphenyl-bridged bis(hydrazine) IV compounds fall in the order $6^+ > 5^+ \gg 10^+$, that is following a $\cos \psi$ instead of the $\cos 2\psi$ relationship observed for the bis-(porphyrins). The bis(hydrazines) have significant CBU-bridge overlap, so that effects transmitted through the π system dominate. Another large difference between the systems is that the zinc porphyrin excited state is both a good oxidant and a good reductant, while the hydrazine cation is only a modest oxidant, and the neutral hydrazine a modest reductant.

An unusually large change in V_{H} with temperature occurs for 5^+ (Table 1). V_{H} increases with temperature very slightly

(14) (a) Heiler, D.; McLendon, G.; Rogalskyj, P. *J. Am. Chem. Soc.* **1987**, *109*, 604. (b) Helms, A.; Heiler, D.; McLendon, G. *J. Am. Chem. Soc.* **1991**, *113*, 4325. (c) Helms, A.; Heiler, D.; McLendon, G. *J. Am. Chem. Soc.* **1992**, *114*, 6227. (d) A significantly larger ψ (50°)^{14c} was estimated by McLendon and co-workers for the **PH**₂-bridged bis(porphyrin) than we estimated for 5^+ ($22-28^\circ$ for $258-298 \text{ K}$). Inclusion of a point for the **PH**₂ system at $\psi = 50^\circ$ would greatly change the appearance of the plot in ref 14b. Reimers and Hush (Reimers, J. R.; Hush, N. S. *Inorg. Chem.* **1990**, *29*, 3686) employ a 32° ϕ angle for biphenyl itself. It seems reasonable that 5^+ would have a smaller ϕ than biphenyl itself, because the hydrazine units are significantly coupled with each other through the bridge in this larger V compound.

(15) Cave, R. J.; Siders, P.; Marcus, R. A. *J. Chem. Phys.* **1986**, *90*, 1436.

for 2^+ and 4^+ (~ 0.5 cal/K), decreases slightly for the highest ϕ compound, 3^+ (-0.7 cal/K), and is unchanged for 6^+ . Because V_H will be proportional to $\cos \phi$ at each N–Ar bond, the small changes indicate that the average ϕ values are not very temperature-sensitive. The temperature coefficient for 5^+ is significantly larger, -3.3 cal/K. 5^+ is the only compound for which temperature can influence overlap within the aromatic system, by changing the average ψ . The ratio of V_H values for $5^+/6^+$ used with a $\cos \psi$ relationship implies that the average ψ for 5^+ increases from 22° to 28° between 258 and 298 K.^{14d}

Dependence of k_{ET} on 1,4-phenylene versus 1,4-naphthylene bridges. Maruyama, Mataga, and co-workers studied the effect of changing from 1,4-phenylene to 1,4-naphthylene bridges for Zn porphyrin, Fe^{III}Cl porphyrin ET in arene-bridged hybrid diporphyrins by fluorescence quenching.¹⁶ They found very similar rate constants, about 0.8×10^{11} and 1.1×10^{11} s⁻¹, respectively. Once again, the result for $\phi \sim 90^\circ$, photo-excited systems forms a contrast to the result for thermal ET in bis(hydrazines). There is considerably faster ET for 1^+ than 4^+ (the rate ratio from optical ΔG^* values at room temperature is 49). The smaller ϕ values for 1^+ and 4^+ make through-bridge coupling important; V is significantly larger for the smaller ϕ compound 1^+ . The result for $1^+/4^+$ result resembles that observed by Staley and co-workers for the same change in bridge, using very different, ion-paired CBU. They recently studied the dipotassium salts of 1,4-dicyclooctatetraenyl-benzene (**A**) and 1,4-dicyclooctatetraenyl-naphthalene (**B**) in THF-d₈, where they exist as (K⁺)₂(COT⁻²)–bridge–(COT⁰) pairs.¹⁷ The rate constant ratio (**A/B**) for two electron and potassium charge transfer that they observed is 166 (at 280 K).

Temperature Dependence of ET Parameters. Hupp and co-workers have studied temperature effects on E_{op} of metal-centered IV–CT complexes. The temperature coefficients (dE_{op}/dT) for the [(NH₃)₅Ru^{III}–NC–Fe^{II}(CN)₅]⁻ → [(NH₃)₅Ru^{II}–NC–Fe^{III}(CN)₅]⁻ IV–CT band varied between -13.5 cm⁻¹ deg⁻¹ in water and -19 cm⁻¹ deg⁻¹ in ethylene glycol.¹⁸ A study on [(bpy)₂ClRu^{II}(pz)Ru^{III}(NH₃)₅]³⁺ prepared under three different conditions gave dE_{op}/dT in CH₃OD of -12 , -10 , and -8 cm⁻¹ deg⁻¹, and under two different conditions in 42:58 propionitrile/butyronitrile, -13 and -7 cm⁻¹ deg⁻¹.¹⁹ In both cases these temperature coefficients were within experimental error of the temperature dependence of ΔG° , estimated from electrochemical measurements on charge-bearing unit models. Because $E_{op} = \lambda + \Delta G^\circ$ for these unsymmetrical IV–CT compounds, this implies a small temperature coefficient for λ . It was thought unlikely that λ_v would exhibit temperature dependence.¹⁸ Using Marcus's expression derived from dielectric continuum theory, λ_s is proportional to the Pekar factor (γ), which depends on the refractive index (n) and static dielectric constant (ϵ_s): $\gamma = 1/n^2 - 1/\epsilon_s$. Dong and Hupp estimated the $d\lambda_s/dT$ contribution in water for an NC-bridged system at ≤ 0.2 cm⁻¹ deg⁻¹.¹⁸ Measured temperature effects on IV–CT bands of symmetrical metal-centered systems that have $\Delta G^\circ = 0$ by symmetry, are indeed small: $+0.1$ (± 0.6) cm⁻¹ deg⁻¹ in water for [(NC)₅-Fe^{II}-(4,4'-bpy)-Fe^{III}(CN)₅],⁵⁻¹⁸ $+1$ (± 1) cm⁻¹ deg⁻¹ in water for [(NH₃)₅Ru^{II}-(4,4'-bpy)-Ru^{III}(NH₃)₅]⁵⁺,¹⁸ and -2 (± 1) cm⁻¹ deg⁻¹ in water for [(bpy)₂ClRu^{II}(pz)Ru^{III}Cl(bpy)₂]³⁺.¹⁹

The data of Table 1 give negative and rather constant dE_{op}/dT values for symmetrical intervalence bis(hydrazines) in acetonitrile: 2^+ $dE_{op}/dT = -3.6$ (± 0.1) cm⁻¹ deg⁻¹, 3^+ -3.7 (± 0.1), 4^+ -4.2 (± 0.1), 5^+ -4.3 (± 0.2), and 6^+ -3.2 (± 0.4). The expected value for $d\lambda_s/dT$ for acetonitrile using the data given by Grampp and Jaenicke²⁰ is $+1.9$ cm⁻¹ deg⁻¹ for $\lambda_s = 10$ kcal/mol. The experimental data show clearly that the Marcus λ_s expression does not predict the right sign for dE_{op}/dT for bis(hydrazine) cations. Matyushov has developed a "molecular" solvent theory incorporating effects of density fluctuations²¹ that does predict the observed sign for $d\lambda_s/dT$ for our compounds, but these calculations will not be discussed here.

Hush treated the increase in bandwidth over $\Delta\nu^{HTL}$ as a measure of $h\nu_v$, using eq 5:^{2b}

$$\Delta\nu_{1/2} = g(\omega, T)\Delta\nu^{HTL} \quad (5a)$$

$$g(\omega, T) = [h\nu_v/2RT \coth(h\nu_v/2RT)]^{1/2} \quad (5b)$$

Although $g(\omega, T)$ for 3^+ drops from 1.31 to 1.26 over the temperature range investigated, the $h\nu_v$ that fits $g(\omega, T)$ rises steadily from 555 cm⁻¹ at 255 K to 642 cm⁻¹ at 327 K. These $h\nu_v$ values seem unreasonably small.⁵ The quartic fit coefficient C describes the increase in bandwidth in the fitting procedure used; $C = 0$ when the observed bandwidth is $\Delta\nu^{HTL}$. C is small and negative at room temperature in acetonitrile for 6^+ (**M₂FL**), which has slightly smaller bandwidth than $\Delta\nu^{HTL}$ despite the fact that it is clearly a localized IV compound. C is negligible for 4^+ (**NA**) and 5^+ (**PH₂**) and significantly positive for the *p*-phenylene-(5- σ bond) bridged compounds, although the order is $3^+ > 1^+ > 2^+$, so C is affected by introduction of methyls but does not correlate with CBU-aryl twisting. C gets slightly closer to 0 as the temperature is increased for these compounds. It also increases upon going from acetonitrile to less polar solvents,^{5,8,12} so the environment is important in addition to the compound's structure. Although it is not clear how to quantify the complex factors that affect C , we think our results demonstrate that the amount of increase in bandwidth over $\Delta\nu^{HTL}$ is not a reliable measure of $h\nu_v$ for these compounds.

Despite E_{op} , $\Delta\nu_{1/2}$, and ϵ_{max} all changing with temperature, V_H evaluated using eq 1 and the quartic fit data for λ and $\Delta\nu_{1/2}$ are nearly constant. Although the expression for V using vibronic coupling theory looks very different from eq 1 because it contains a Franck–Condon factor instead of $\Delta\nu_{1/2}$,¹³ it is numerically very close to V_H except for the introduction of dependence on the refractive index of the solvent (n).^{12a} The n factor is designed to correct for an increase in ϵ in the solvent cavity containing the compound studied.^{13,22} Written for the classical theory used here, the corrections used result in $V = V_H/n^{1/2}$ ($0.86V_H$ for acetonitrile at room temperature),¹³ or in a later paper $V = V_H[9n^2/(n\{n^2 + 2\})]^{1/2}$ ($0.91V_H$ for acetonitrile at room temperature) with a caution that the correction might be more complicated than this.²²

Optical and Thermal ET Barriers. The thermal ET barriers estimated from the optically derived parameters calculated as described above^{5,8} were in used eq 6 to calculate k_{OPT} , the predicted value of the thermal ET rate constant derived from

(20) Grampp, G.; Jaenicke, W. *Ber. Bunsen-Ges. Phys. Chem.* **1991**, *95*, 904.

(21) (a) Matyushov, D. V. *Mol. Phys.* **1993**, *79*, 795. (b) Matyushov, D. V. *Chem. Phys.* **1993**, *174*, 199. (c) Matyushov, D. V.; Schmid, R. J. *Phys. Chem.* **1994**, *98*, 5152. (d) Matyushov, D. V.; Schmidt, R. *Chem. Phys. Lett.* **1994**, *220*, 369.

(22) Gould, I. R.; Young, R. H.; Mueller, L. J.; Albrecht, A. C.; Farid, S. *J. Am. Chem. Soc.* **1994**, *116*, 3147.

(16) Osuka, A.; Maruyama, K.; Mataga, N.; Asahi, T.; Yamazaki, I.; Tamai, N. *J. Am. Chem. Soc.* **1990**, *112*, 4958.

(17) Staley, S. W.; Kehlbeck, J. D.; Grimm, R. A.; Sablosky, R. A.; Boman, P.; Eliasson, B. *J. Am. Chem. Soc.* **1998**, *120*, 9793.

(18) Hupp, J. T.; Dong, Y. *Inorg. Chem.* **1992**, *31*, 3322.

(19) Hupp, J. T.; Neyhart, G. A.; Meyer, T. J.; Kober, E. M. *J. Phys. Chem.* **1992**, *96*, 10820.

Table 4. Comparison of Optical and Thermal ET Barriers in Acetonitrile

cmpd	bridge	optical ^a			ESR	
		$\Delta G^\ddagger(25^\circ\text{C})$ (kcal mol ⁻¹)	ΔH^\ddagger (kcal mol ⁻¹)	ΔS^\ddagger (cal mol ⁻¹ K ⁻¹)	ΔH^\ddagger	ΔS^\ddagger
2 ⁺	XY	5.47	6.3 ± 0.2	+2.8 ± 0.6	2.7 ± 0.4	-9.5 ± 0.2
3 ⁺	DU	5.24	5.1 ± 0.2	-0.5 ± 0.7	4.8 ± 0.2	-1.8 ± 1.0
4 ⁺	NA	4.66	5.7 ± 0.2	+3.6 ± 0.5	2.7 ± 0.7	-8.0 ± 3.9
5 ⁺	PH ₂	6.77	5.0 ± 0.4	-5.8 ± 1.4	3.5 ± 0.1	-10.9 ± 0.4
6 ⁺	M ₂ FL	5.60	6.7 ± 0.2	+3.6 ± 0.8	3.9 ± 0.1	-5.5 ± 0.4

^a Calculated using eq 5, with $\lambda_v = 25$ kcal/mol for **2**⁺, **3**⁺, and **5**⁺, and 20 for **4**⁺ and **6**⁺; the results are quite insensitive to the λ_v employed.

the optical spectrum, using $h\nu_v = 800$ cm⁻¹ ($\nu_v = 2.40\text{H}10^{13}$ s⁻¹).

$$k_{\text{OPT}} = \nu_v(\lambda_v/\lambda)^{1/2} \exp(-\Delta G^*/k_{\text{B}}T) \quad (6)$$

The $(\lambda_v/\lambda)^{1/2}$ term is close to constant and does not affect k_{OPT} significantly. Table 4 compares thermal and optical rate constants for **2**⁺–**6**⁺ in the form of Eyring activation parameters, and Figure 2 shows the data graphically. It may be noticed that the optical enthalpies of activation ($\Delta H^\ddagger(\text{opt})$) are rather constant but that there is a large range of ESR-derived $\Delta H^\ddagger(\text{esr})$ values. There appears to be less experimental error in obtaining $\Delta H^\ddagger(\text{opt})$ because both the optical band shape is far simpler than that for the very complex ESR spectra and the simulations fit the experimental curves better. The best agreement between optical and ESR data occurs for **3**⁺. The ESR data should be best for **3**⁺, which has the smallest ring-splitting constants in the frozen form. We cannot freeze out the ring splittings in the ESR spectrum and do not know the value to use for the frozen spectrum in the simulations.⁵ The k_{ESR} values are most accurate at the temperature of maximum broadening, which is roughly the center of the temperature range for which data are reported, because the line shape changes with changes in k_{ESR} are largest at this point. Only a small temperature range is available for k_{ESR} , limiting the accuracy of the activation parameters that can be extracted. In contrast, the optical band shape fits are comparable at all temperatures reported. We suggest that the very negative $\Delta S^\ddagger(\text{esr})$ values (and accompanying smaller $\Delta H^\ddagger(\text{esr})$ values) found for **2**⁺, **4**⁺, and **5**⁺ are likely to be inaccurate and that activation parameters estimated from the optical spectrum are likely to be more accurate than those from ESR.

The poorest agreement between k_{OPT} and k_{ESR} is for the fluorenyl-bridged compound **6**⁺, for which taking optical data was stopped at 298 K because decomposition became obvious at higher temperatures, and for which an experimental estimate of d is not available. Nevertheless, extrapolating k_{OPT} to the extreme temperatures of the ESR data set gives rate constant ratios $k_{\text{ESR}}/k_{\text{OPT}}$ of 1.5 at 273.1 K and 2.5 at 248.1 K. There is excellent agreement between the ESR rate constants and the optical data treated the way we did above for all five compounds. Lowering the V used by including refractive index corrections in calculating it from the optical spectrum and raising λ by using the vibronic coupling theory concept of fitting reduced spectra^{11,13} would both lower k_{OPT} , making agreement with experiment poorer for four of the five compounds studied. However, the uncertainty in d appears to us to preclude definitely determining whether it is better to use a smaller value than the V_{H} we used to fit experimental data. The change in the effective distance found for d_{esr} as methyls introduced on the **PH** bridge could be caused by change in CBU-bridge interactions that are not accounted for in the two-state model.

Difficulties in Separation of λ_v from λ_s . Accurate calculation of k_{ET} for **2**⁺–**6**⁺ from their CT bands does not require separation of λ into λ_v and λ_s , and the IV–CT band shape does

not allow such separation either. But application of vibronic coupling theory requires accurate separation of λ into λ_v and λ_s , so we consider here making such separation by comparing λ values for the compounds studied. Despite constant CBU, rather similar bridges, and ET distances that are “known” (in the sense that using those in footnote d of Table 1 produces estimated V values from the IV–CT bands that accurately reproduce the experimental rate constants), accurate separation of λ into its components from our experimental data does not appear to us to be possible. The change in λ as methylenes are added to the bridge in the series **1**⁺ → **2**⁺ → **3**⁺ (37.8 → 41.15 → 40.65 at room temperature) indicates compensating effects on λ_v and λ_s as methylation increases.⁵ Adding methyl groups increases ϕ . This increases λ_v (twisting at the N–Ar bond significantly destabilizes a radical cation), but it also decreases λ_s . The d value we used increases significantly upon increasing twist, but prediction of the effect on λ_s is hard to quantify because the effective radius (r) of the CBU presumably decreases; less spin density appears in the p -phenylene ring, causing the increase in d . For **1**⁺ → **5**⁺ and **6**⁺, there is an obvious increase in d , and ϕ is presumably rather similar for these three compounds because the hydrazine units are flanked by ortho hydrogens in all three cases. Although λ_s increases for **5**⁺ by 5.7 kcal/mol, this increase is significantly smaller than the 16.1 kcal/mol that would be predicted by making the usual dielectric continuum theory assumption for intervalence compounds that $\lambda_s = e^2(r^{-1} - d^{-1})\gamma$. It is not surprising that a deviation occurs, because d is probably not $>2r$ for **1**⁺, which is an assumption in deriving the λ_s formula.² Even the obvious increase in d between **1**⁺ and **6**⁺ does not lead to an increase in λ but a decrease of 0.2 kcal/mol. We suggest that this indicates that methylation on the bridge lowers λ_s , even in the absence of the increase in ϕ that accompanies methylation for **1**⁺–**3**⁺.

Conclusion

The treatment we used for predicting the thermal electron-transfer rate constant from optically derived ET parameters (k_{OPT}) differs from the Marcus–Hush treatment in two significant ways. We use Hush’s eq 1 to estimate V but have altered the ET distance d that we employed in applying it. We used an experimental estimate of the ET distance on the adiabatic surface (d_{esr}), using the 2+ oxidation state as a model for the 1+ intervalence oxidation state. This resulted in a 23% increase in d as methyls are substituted on a p -phenylene bridge in **1**⁺, **2**⁺, and **3**⁺. Hush theory employs the distance on the diabatic surfaces, which ought not to change because the distance between the charge-bearing units does not change significantly as methyls are introduced. Second, we have made no attempt to explicitly include vibronic coupling theory in obtaining the intervalence charge-transfer band shape. Instead, we assumed that this band shape reveals the shape of the adiabatic surfaces on which thermal electron transfer occurs and that the simplest two-state model suffices. We show that the band shape can be

transformed into the diabatic potential-energy surface unambiguously, by demonstrating that very different functions taken to describe the diabatic potential-energy surfaces give almost identical ΔG^* values for the adiabatic surfaces in the transformation. Our treatment increasingly lowers the diabatic surface-crossing energy from the $E_{op}/4$ for parabolic diabatic surfaces as the bandwidth increases over the eq 2 $\Delta\nu^{HTL}$ value. Using our model, eq 4 is an excellent estimate of the thermal ET barrier (ΔG^*). With these modifications to Marcus–Hush theory, eq 6 produces k_{OPT} values as a function of temperature that are in very good agreement with rate constants determined by ESR for $2^+ - 6^+$. Our simplified treatment obviously does not allow insight into how the adiabatic surfaces arise in terms of vibronic coupling theory. A complex treatment involving many parameters would be required to apply vibronic coupling theory properly for our high λ_v compounds.

Acknowledgment. We thank the National Science Foundation for support of this work under grant CHE-9417946, the NSF major instrument program and the University of Wisconsin for funds used in purchase of the diffractometers, spectrometers, and computer equipment used, and the Dow Chemical Company for a fellowship for R.F.I. We thank Dmitry Matyushov for discussion of temperature coefficients using his solvent theory.

Supporting Information Available: Crystallographic data for **5⁰**, **5²⁺**(SbF₆⁻)₂·CH₃CN, **8⁺**(SbF₆⁻)·1/2Et₂O, and **9⁺**(SbF₆⁻), numbered thermal ellipsoid drawings, heavy atom positions, and experimental for preparation of **4**, **5**, **6**, **8**, **9**, **10**, and their radical cations. This material is available free of charge via the Internet at <http://pubs.acs.org>.

JA984047K